The Journal of Neuroscience, January 1, 1997, 17(1):32–44

A Novel Subunit for Shal K^+ Channels Radically Alters Activation and Inactivation

Timothy Jegla and Lawrence Salkoff

Department of Anatomy and Neurobiology, Washington University School of Medicine, St. Louis, Missouri 63110

Shal (Kv4) potassium channel genes encode classical subthreshold A-currents, and their regulation may be a key factor in determining neuronal firing frequency. The inactivation rate of Shal channels is increased by a presently unidentified class of proteins in both *Drosophila* and mammals. We have cloned a novel Shal channel subunit (jShalγ1) from the jellyfish *Polyorchis penicillatus* that alters Shal currents from both invertebrates and vertebrates. When co-expressed with the conserved jellyfish Shal homolog jShal1, jShalγ1 dramatically changes both the rate of inactivation and voltage range of activation and steady-state inactivation. jShalγ1 provides fast inactivation by a classic N-type mechanism, which is independent of its effects on voltage dependence. jShalγ1 forms functional channels only as a heteromultimer, and jShalγ1 + jShal1 heteromultimers are functional only in a 2:2 subunit stoichiometry.

Key words: K^+ channel; Shal; inactivation; Polyorchis*; a-current; heteromultimer; jellyfish; diploblast; γ-subunit*

Transient K^+ currents that are active at subthreshold potentials (A-currents) (Connor and Stevens, 1971a) are a dominant K^+ conductance during the interspike interval and have a major influence on the firing frequency of neurons (Connor and Stevens, 1971b). Of the four subfamilies of genes that encode the channel-forming α-subunits of voltage-gated K^+ channels (Shaker, Shab, Shal, and Shaw), the Shal (Kv4) subfamily most closely matches the description of the classical subthreshold A-current. The importance of subthreshold A-currents is underscored by the fact that Shal is the most highly conserved voltage-gated K^+ channel subfamily in higher triploblastic metazoans (Salkoff et al., 1992).

Recent genetic and molecular evidence supports the idea that Shal channels underlie classical subthreshold A-currents in neurons of both vertebrates and invertebrates. Serodio et al. (1994) have shown that the major subthreshold A-current expressed in the rat brain is likely to be encoded by Shal genes. Shal channels in the mammalian brain are located primarily on the dendrites and cell bodies of neurons (Sheng et al., 1992), where their placement might influence spiking behavior. Using mutant analysis, Tsunoda and Salkoff (1995a,b) also found Shal currents in cell bodies of neurons from the fruit fly *Drosophila*, suggesting that the intracellular location and function of these channels is conserved across species.

Shal inactivation rate is regulated by an unknown mechanism in both vertebrates and *Drosophila*. Shal currents vary almost 50-fold in inactivation rate in *Drosophila* embryonic neurons. Most *in vivo* Shal currents inactivate far more rapidly than currents expressed when Shal cRNA is injected into *Xenopus* oocytes (Pak et al., 1991). In mammals, the inactivation rates of Shal currents can be increased by co-expression in *Xenopus* oocytes with low molecular weight fractions of mRNA from rodent brain (Chabala et al., 1993; Serodio et al., 1994). Both results suggest a mechanism for increasing the rate of inactivation in Shal channels that is not intrinsic to Shal α-subunits. Because Shal currents influence the duration of the interspike interval (Connor and Stevens, 1971b), their inactivation rates may determine neuronal firing patterns. Thus, understanding the mechanism controlling Shal inactivation rates may be important for understanding how neuronal firing patterns are generated.

We have explored the evolutionary origins of Shal channels in a primitive metazoan and have discovered a molecular mechanism for regulating the inactivation rate of Shal currents. We show here that Shal is highly conserved in the jellyfish *Polyorchis penicillatus*, a diploblastic coelenterate. Because diploblasts are the most primitive metazoans to have nervous systems, our results show that Shal currents were present in the first neurons that evolved in the last common ancestors of diploblasts and triploblasts, ~700 million to 1 billion years ago (Morris, 1993). One *Polyorchis* Shal homolog, jShalγ1, appears to function only as a heteromultimer in concert with a Shal α-subunit. Compared with homomultimeric Shal channels consisting of Shal α-subunits alone, Shalα + Shalγ heteromultimers produced currents that inactivate far more rapidly. In contrast to the cytosolic β-subunits that provide rapid inactivation in mammalian Shaker K^+ channels (Rettig et al., 1994), jShalγ1 is homologous to the α-subunits of voltage-gated K^+ channels.

MATERIALS AND METHODS

Cloning. Amplification and isolation of fragments of *jShal1* and *jShalγ1* from *Polyorchis penicillatus* genomic DNA was performed as described in Jegla and Salkoff (1995) and Jegla et al. (1995). Briefly, the degenerate primers 5′-TCGGAATTCTATGACTACTGTTGGNTAYGGNGA-3′ and 5′-ACCTCTAGAGGTAGTGCTATTRYNAGNACNCC-3′, which are derived from the consensus amino acid sequences of the P-domain (MTTVGYGD) and the S6 domain (GVL(T/V)TIAL) of voltage-gated K^+ channels, were used to amplify initial fragments. These were size-

Received July 11, 1996; revised Sept. 17, 1996; accepted Oct. 7, 1996.

This research was supported by a grant from National Institutes of Health and the MDA to L.B.S. We especially thank Dr. Warren Gallin (University of Alberta) and Dr. Andrew Spencer (Bamfield Marine Station and University of Alberta) for providing the *Polyorchis* libraries and genomic DNA. We also thank Alice Butler, Michael Pak, and Jim Ray for their work in determining intron positions in dShal and mShal.

Correspondence should be addressed to Prof. Lawrence B. Salkoff, Department of Anatomy and Neurobiology, Washington University School of Medicine, 660 South Euclid Avenue, P.O. Box 8108, St. Louis, MO 63110.

Dr. Jegla's current address: Department of Molecular and Cellular Physiology, Stanford University School of Medicine, Palo Atlo, CA 94305.

 0270-6474/96/170032-13$05.00/0

selected, reamplified using overlapping nondegenerate primers, and then subcloned to allow for isolation of individual fragments.

A complete *jShal1* genomic clone was obtained using the initial *jShal1* fragment to probe a *Polyorchis* genomic library (provided by Dr. Warren Gallin, University of Alberta) under high-stringency conditions (Butler et al., 1989) and sequenced. The coding region of *jShal1* consists of three exons, as indicated in Figure 1. Two exons encoding the N-terminal, S1–S6, and neighboring C-terminal cytoplasmic regions were predicted based on their high homology to dShal and mShal. The third exon encoding the poorly conserved distal C-terminal region was identified by amplification from an oligo dT-primed *Polyorchis* cDNA library using a *jShal1*-specific sense primer in the S6 region (5′-CCTGGTAAACTA-GTTGGTAGTATTTGCTCA-3′) and an antisense primer corresponding to the library vector sequence (5′-TCCGGTCGACGTAGAGGG-GAATAAATCGCCATA-3′). Construction of the *Polyorchis* genomic library and of cDNA libraries from neuronally enriched *Polyorchis penicillatus* tissue samples have been described previously (Gallin, 1991).

The *jShalγ1* genomic sequence was obtained in two sequential rounds of inverse PCR (Ochman et al., 1988). The genomic DNA used for inverse PCR was prepared by first cutting with a desired restriction enzyme and then ligating at concentrations of 2 ng/μl or less to promote self-circularization. In the first round of inverse PCR, a 1.4 kb fragment of *jShalγ1* was amplified from DNA prepared with *Bgl*II using sense (5′-CAAGTCTAGATGATAGGCTCTATGTGTTGCTTGAT-3′) and antisense (5′-AACTAAGCTTGGATGGTAACAGGAACAACATC-3′) primers derived from the original P-domain–S6 *jShalγ1* fragment. Sequencing revealed that the fragment included a *Bgl*II site at the beginning of S2 and extended through the 3′ end of the open reading frame. Inverse PCR was also performed on genomic DNA prepared with *Hin*dII using *jShalγ1*-specific primers (5′-CAGTTGTTTAGTTATAACCCTCTCC-3′) and (5′-GCCAAAGAAAAGGTGGGGTCTTCAC-3′) located 5′ of a *Hin*dII site in S3. A 900 bp fragment obtained in this screen was found to extend through the 5′ end of jShalγ1 coding sequence. The 3′ coding region of *jShalγ1* was confirmed by PCR amplification from a *Polyorchis* cDNA bank by the same method as for *jShal1*, but with the *jShalγ1*-specific sense primer used in the first round of inverse PCR. A stop codon was found just 3′ of S6 in two cDNAs and is also present in the genomic sequence. The 5′ coding region was not found in any cDNA clones but was instead determined from genomic sequence. Our analysis, based on several observations, indicated that no introns interrupt coding in this region. First, no consensus sequences for acceptor or donor splice junctions were found in this region. Second, the codons used in this predicted 5′ region of *jShalγ1* match the coding bias we have observed for six *Polyorchis* K^+ channel genes (data not shown). Finally, this region has an A/T content of 64%, which falls within the range we have observed for *Polyorchis* coding sequence (60–65%), but well below the range we have observed for *Polyorchis* introns (72–76%).

Alignments and phylogenetic trees. The amino acid alignment (see Fig. 1) was generated using Microgenie (Beckman, Palo Alto, CA) and optimized by eye. Phylogenetic trees were constructed from these alignments by maximum parsimony, as implemented in the PAUP computer program (Swofford, 1993). Only sections of the T1 region and membrane spanning core (S1–S6) that have relatively conserved lengths (and thus certain alignment) among the Shaker, Shal, Shab, and Shaw subfamilies were used for tree building. Tree lengths were calculated using a step matrix that weighted changes between amino acids according to the minimum number of nucleotide changes that were necessary to achieve the change. A heuristic search for optimal trees was performed using random addition to generate initial trees. Tree bisection and reconnection were then used to optimize the trees. The consensus maximum parsimony tree (see Fig. 2) was constructed from the 18 shortest trees found in this search.

Expression vector construction. The complete open reading frame of *jShal1* was united by removing the two introns from the genomic clone. The 3′ intron was removed from *jShal1* in two subcloning steps. First, the C-terminal cDNA fragment (which spanned from S6 to the C terminal) was subcloned into Bluescript II SK^+ (Stratagene, La Jolla, CA) using an *Spe*I site in S6 and an *Eco*RI site from the cDNA library vector. Second, a genomic fragment spanning from an *Xba*I site 5′ of the initiator methionine to the *Spe*I site in S6 was cloned into the *Spe*I site of this cDNA subclone. The P-domain intron was removed using overlap extension PCR off this template (Ho et al., 1989). The final overlap extension product was produced using a sense primer (5′-TTACGAATTCG-CCACCATGAAT GGTGACATAGGCGCTT-3′) that adds a consensus translation initiation sequence (underlined) (Kozak, 1987) surrounding the *jShal1* initiator methionine and an antisense primer from the Bluescript vector. This product was cut with *Eco*RI and cloned into the *Eco*RI site of the *Xenopus* oocyte expression vector pBSMXT (Wei et al., 1994). The coding region was then sequenced and compared with the *jShal1* genomic clone to confirm that no PCR-introduced mutations existed.

A similar overlap extension protocol was used to remove both introns from the open reading frame of jShalγ1. The final product was made with a sense primer (5′-ATATGGATCCACCATGTATTCGGTTACTTC-CACTGCAAC-3′) that introduced a consensus translation initiation sequence (underlined) to the jShalγ1 initiator methionine and an antisense primer (5′-CTTATCTAGATCAATCTTCTTCGCTAGCCTTCA-TTTGAATTATTGGGACAGG-3′) that includes the jShalγ1 stop codon and spans coding sequence on both sides of the 3′ intron. It was cut at flanking *Bam*HI and *Xba*I sites introduced in the primers and subcloned into the pOX expression vector. Four individually amplified clones were sequenced and compared with each other as well as with the original inverse PCR-generated jShalγ1 clones, allowing PCR-introduced mutations to be identified. A jShalγ1 expression vector clone containing two silent mutations was used in all physiological experiments. The pOX vector was constructed by inserting *Xenopus* β-globin 5′ and 3′ untranslated sequences contained in pBSMXT (Wei et al., 1994) into new restriction sites in pBluescript II KS+ (Stratagene). Briefly, the *Xenopus* β-globin 5′ untranslated and an *Nhe*I site was inserted between the *Kpn*I and *Sal*I sites of the vector, while an *Xho*I site and the *Xenopus* β-globin 3′ untranslated were inserted between the *Xba*I and *Not*I sites.

Expression and electrophysiology. Capped cRNAs were prepared by run-off transcription with T3 RNA polymerase using the mMessage mMachine kit (Ambion, Austin, TX) and diluted in RNase-free ddH_2O to desired concentrations before injection. Mature stage IV *Xenopus* oocytes were prepared for injection as described in Wei et al., 1990. Oocytes were injected with 50 nl of cRNA and incubated at 18°C for 1–5 d in ND96 containing (in mM): 96 NaCl, 2 KCl, 1.8 $CaCl_2$, 1 $MgCl_2$, 5 HEPES–NaOH, pH 7.5, supplemented with 100 U/ml penicillin, 100 μg/ml streptomycin, and 2.5 mM sodium pyruvate. Recording methods used were as published previously in Covarrubias et al., 1991. Briefly, whole-cell recordings were made 1–5 d after injection at room temperature (~22°C) by conventional two-microelectrode voltage-clamp techniques. Electrodes ranged from 0.2 to 0.5 MΩ in resistance and were filled with 3 M KCl. The standard recording solution consisted of ND96 with 1 mM 4,4′-diisothiocyanatostilbene-2,2′ disulfonic acid to block native oocyte chloride currents. Currents were digitally acquired with CCURRENT using linear leak subtraction, filtered at 1 kHz with an eight-pole Bessel filter and analyzed with CQUANT. Capacitative transients were removed by leak subtraction or clipped out.

Stoichiometry calculations. Time constants (see Fig. 7) were calculated by least-squares fits of double-exponential functions to traces like those shown in the insets. Because the slowly inactivating jShal1 current could be inactivated by a prepulse to −90 mV, such a prepulse was often used to help isolate the fast components produced by jShal1 + jShalγ1 heteromultimers in oocytes expressing both currents. The free-mixing curve shown in Figure 7 assumes a binomial distribution of channels containing zero to four jShalγ1 inactivation balls. If p equals the fraction of jShal1 subunits and q equals the fraction of jShalγ1-subunits, then the distribution of channel types is as follows: p^4 (0 balls) + p^3q (1 ball) + p^2q^2 (2 balls) + pq^3 (3 balls) + q^4 (4 balls). The fractional size of the slowly inactivating current (jShal1 homomultimers, 0 balls) represents p^4 and could thus be used to predict the fraction of each type of channel. The predicted fast-inactivation time constants were obtained by adjusting the inactivation rate constant calculated for these currents to the average number of inactivation balls per channel predicted from the binomial distribution of channel types. Only those channels containing one to three balls were included in the calculations of the fast-inactivation time constants, because channels with four balls (jShalγ1 homomultimers) are nonfunctional. Thus, if free mixing occurs, the fastest inactivation time constants observed in jShalγ1-biased currents with no jShal1 homomultimeric fraction (2.69 msec) should be produced primarily by channels with three inactivation balls. Thus, the time constant of fast N-type inactivation should approach three times this value as the proportion of jShal1 is increased. The equations for calculating inactivation rate constants from the time constants of inactivation and recovery and for calculating the free mixing curve are from MacKinnon et al., 1993.

The time constants (see Fig. 8) were determined by triple exponential fits to current traces like those shown in the insets, because two time constants of slow inactivation (from jShal1 + jShalγ1(T) heteromultimers) contributed to the accuracy of the fit. The curve for the

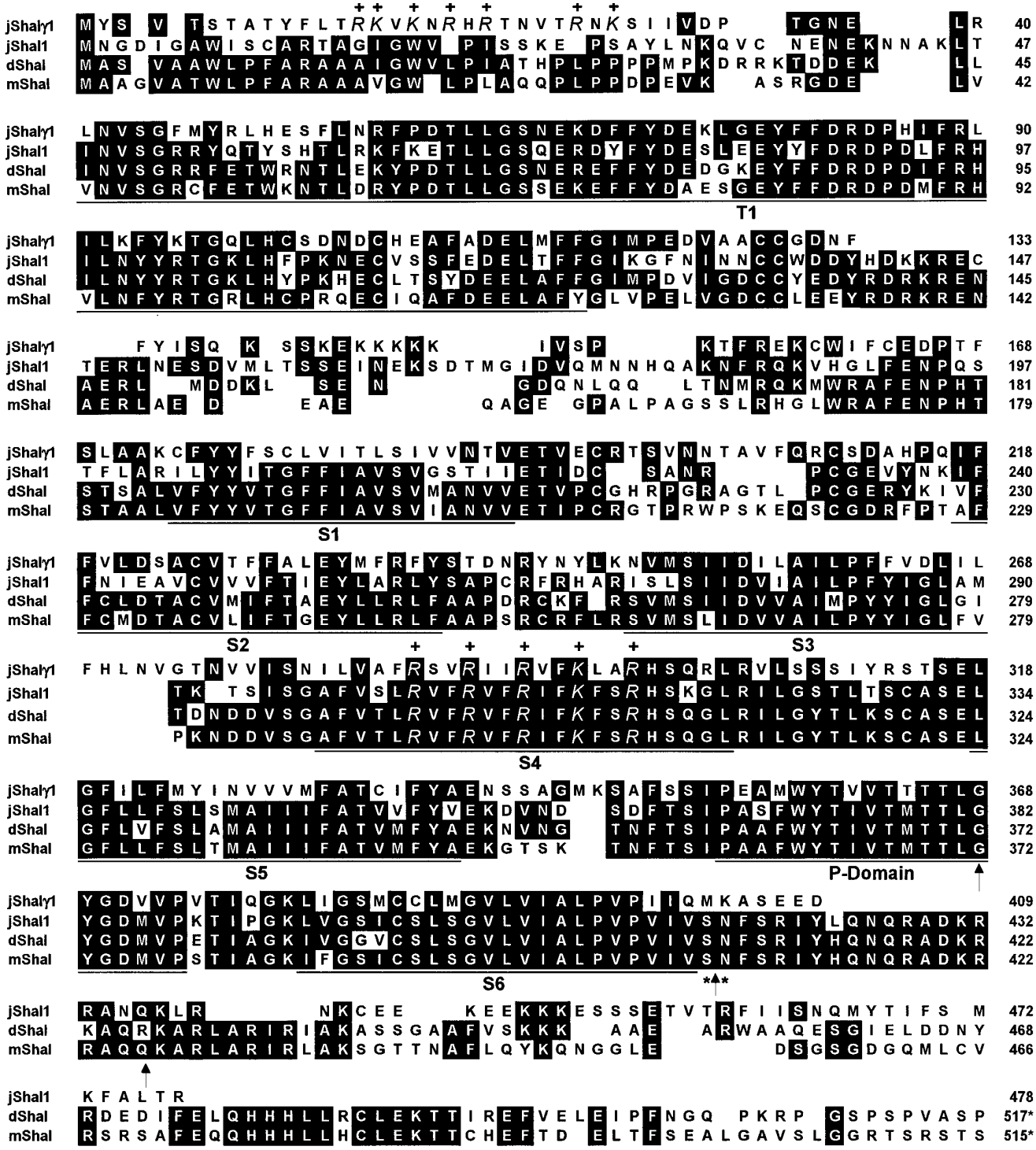

Figure 1. jShal1 and jShalγ1 amino acid sequences. Jellyfish Shal homologs jShal1 and jShalγ1 are compared with Shal channels from *Drosophila* (dShal; Wei et al., 1990) and mouse (mShal, Kv4.1; Pak et al., 1991). Identical residues are shown in reversed lettering (*white on black*). Predicted transmembrane domains (S1–S6) and a K^+ channel pore motif (P-domain; Hartmann et al., 1991; Yool and Schwarz, 1991) are *underlined*. Also *underlined* is the cytoplasmic N-terminal domain (T1), which is believed to mediate subfamily-specific assembly of voltage-gated K^+ channel subunits (Li et al., 1992; Shen et al., 1993; Shen and Pfaffinger, 1995). *Large italic letters* and *plus symbols* mark five evenly spaced positively charged residues found in S4 voltage sensor (Papazian et al., 1991) and seven positively charged residues near the N terminal of jShalγ1 that are part of a motif similar to N-terminal inactivation ball motifs (Murrell-Lagnado and Aldrich, 1993). The positions of two introns conserved in jShal1, dShal, and mShal are marked with *arrows*. Of these two, only the intron position in the P-domain motif is also found in jShalγ1. A third jShalγ1-specific intron near S6 is labeled with an *arrow bracketed* by *asterisks*. Residue numbers are shown on the *right*. *Asterisks* by the residue numbers at the end of the dShal and mShal sequences indicate that they are incomplete. The GenBank accession numbers for *jShal1* and *jShalγ1* are U78642 and U78641, respectively.

Table 1. Percent amino acid identity shared between jellyfish Shal homologs, triploblastic Shal homologs, and a jellyfish Shaker homolog

	jShal1	jShalγ1	dShal	mShal	jShak1
jShal1	–	41 (52)	66 (64)	65 (51)	40 (37)
jShalγ1	41 (52)	–	42 (51)	44 (51)	33 (32)
dShal	66 (64)	42 (51)	–	83 (67)	43 (36)

Percent amino acid identities are shown for pairwise alignments between jShal1, jShalγ1, the *Drosophila* Shal homolog dShal (Wei et al., 1990), the mouse Shal homolog mShal or Kv4.1 (Pak et al., 1991), and the jellyfish Shaker homolog jShak1 (Jegla and Salkoff, 1995). Identities are measured from the first residue of S1 to the last residue of S6 and for the most highly conserved regions surrounding the T1 domain corresponding to amino acids 39–133 of jShal1 (shown in parentheses).

prediction ofchannels containing three jShalγ1-subunits assumes that four types exist, all heteromultimers with three jShalγ1-based-subunits and one jShal1-subunit, but with zero to three inactivation balls. Because of the high ratio of jShalγ1 and jShalγ1(T) to jShal1 used in these experiments, few jShal1 homomultimers are predicted to exist, allowing these channels to be excluded from the calculations. If p equals the fraction of jShalγ1(T)-subunits and q equals the fraction of jShalγ1-subunits, then the distribution of channel types is: p^3 (0 balls) + p^2q (1 ball) + pq^2 (2 balls) + q^3 (3 balls). The fraction of slowly inactivating current (p^3) was used to calculate the fraction of each channel type. For the prediction of two jShalγ1-subunits in each channel, the distribution is simplified to three possible channel types: p^2 (0 balls) + pq (1 ball) + q^2 (2 balls). In this case, the slowly inactivating current fraction equals p^2. For the prediction of a single jShalγ1-subunit, just two channel types will exist, p and q, and the slowly inactivating current fraction equals p. The curves were again calculated by the method of MacKinnon et al. (1993) but with the binomial distributions explained above.

RESULTS

Cloning and conservation

A previous study of the evolutionary origins of voltage-gated K^+ channels showed that homologs of mammalian channels are present in the jellyfish *Polyorchis penicillatus*, which is among the simplest extant metazoans to have an organized nervous system (Jegla et al., 1995). We infer from this result that a similar set of voltage-gated K^+ channels play an indispensable role in the nervous systems of all metazoans. Shal is the most conserved among these channels in the higher triploblastic metazoa, and here we describe highly conserved *Polyorchis* Shal homologs, *jShal1* and *jShalγ1*. Because regulation of Shal channels may be a key element in the generation of patterned neuronal output, we have now focused attention on the mechanism of this regulation, which may be conserved as well.

jShal1 and jShalγ1 gene fragments were initially isolated by a PCR screen of *Polyorchis penicillatus* genomic DNA. Degenerate primers for this screen were based on regions of the P-domain (MTTVGYGD) and S6 transmembrane domain (GVL(T/V)IAL) that are highly conserved among voltage-gated K^+ channels. The P-domain–S6 fragments of *jShal1* and *jShalγ1* were used to isolate complete coding sequences for these genes both by hybridization and PCR techniques, as described in Materials and Methods. Figure 1 shows the deduced amino acid sequences of the jShal1 and jShalγ1 proteins compared with the sequences of Shal proteins from the fruit fly *Drosophila* (dShal) and mouse (mShal, Kv4.1). Each contains the characteristic structural features of voltage-gated K^+ channel α-subunits.

jShal1 is very clearly a direct homolog of triploblastic Shal genes, because the jShal1 protein shares high conservation to triploblastic Shal α-subunits over virtually its entire length. It is ~65% identical to dShal and mShal across the membrane-spanning channel core (Table 1). Interspecies homologs of specific voltage-gated K^+ channel genes typically share at least 50% amino acid identity over this region, and jellyfish and triploblastic Shaker homologs share only this 50% amino acid identity (Jegla et al., 1995). The higher level of conservation in jShal1 is consistent with previous observations that Shal is the most highly conserved subfamily of voltage-gated K^+ channels (Salkoff, 1992). Conservation is nearly as high in the T1 domain, which mediates subfamily-specific channel assembly (Li et al., 1992; Shen et al., 1993; Shen and Pfaffinger, 1995). *jShal1* also has a conserved genomic structure; the positions of two introns, one in the P-domain motif and one in the C-terminal cytoplasmic domain, are perfectly conserved among *jShal1*, *dShal*, and *mShal* (Fig. 1, *arrows*).

In contrast, jShalγ1 is less well conserved and shares barely >40% amino acid identity from S1 to S6 (Table 1). Despite this lower conservation, several lines of evidence lead us to put *jShalγ1* in the Shal K^+ channel subfamily. As with all Shal α-subunits, *jShalγ1* contains an intron at the "Shal-specific" site in the P domain. Introns are not found at this position in genes from the Shaker, Shab, or Shaw subfamilies. Secondly, Shal-specific conservation is high (>50%) in the T1 subfamily-specific assembly domain. Finally, phylogenetic analysis of jShal1, jShalγ1, and 15 other voltage-gated K^+ channel proteins representing the Shaker, Shab, Shal, and Shaw subfamilies unequivocally places jShalγ1 within the Shal subfamily. A consensus of the 18 shortest trees found in a heuristic search using maximum parsimony (PAUP, Swofford, 1993) is shown in Figure 2. jShalγ1 is placed within the Shal subfamily in all of these trees. The order of branching between channel subfamilies shown in Figure 2 is not consistent in these 18 trees and should not be taken to indicate the evolutionary relationships of these subfamilies.

The lower conservation shared between jShalγ1 and Shal α-subunits is especially evident in the S4 voltage sensor (Papazian et al., 1991), which is perfectly conserved between dShal and mShal and has only two substitutions of 22 residues in jShal1. In contrast, there are 12 substitutions in the same 22 residues of jShalγ1 (Fig. 1). Interestingly, these S4 differences are found in the hydrophobic residues, whereas the string of positively charged residues characteristic of S4 is identical.

Two other key features distinguish jShalγ1 from jShal1 and other Shal homologs. One is that jShalγ1 has a group of seven positively charged residues at near its N terminal that is not found in other Shal homologs (Fig. 1). This motif is reminiscent of an inactivation "'ball," similar to those responsible for rapid inactivation in both triplobastic and diploblastic Shaker channels (Hoshi et al., 1990; Zagotta et al., 1990; Jegla et al., 1995). Later, we will show that these charges are indeed part of a functional inactivation ball in channels containing jShalγ1. The second feature is that after S6, jShalγ1 has a segment of just seven amino acids and thus lacks a long conserved C-terminal cytoplasmic segment found even in jShal1 (Fig. 1).

Expression

Shal1 expresses a rapidly activating transient current in *Xenopus* oocytes that resembles Shal currents from *Drosophila* and mammals. Figure 3 shows a comparison of the jShal1 current and the *Drosophila* Shal current dShal. The biophysical properties of these two currents are summarized in Table 2. Both currents share features of classic subthreshold A-currents that distinguish Shal currents from other voltage-dependent K^+ currents. These include a hyperpolarized steady-state inactivation curve and an

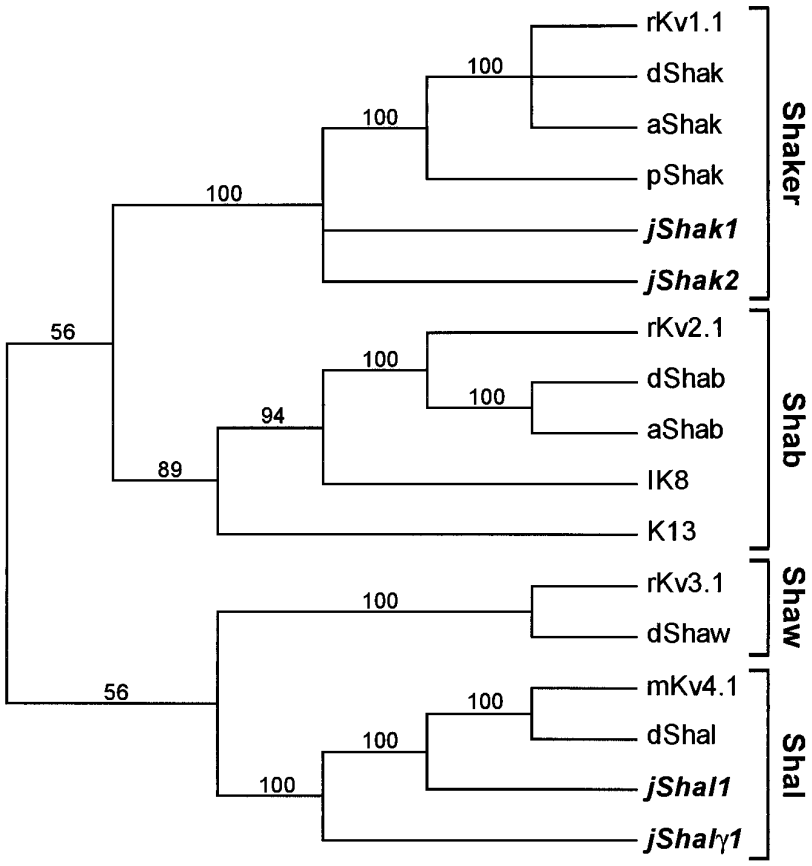

Figure 2. Phylogenetic analysis places jShal1 and jShalγ1 in the Shal subfamily. A consensus maximum parsimony tree of jShal1, jShalγ1, and 15 voltage-gated K^+ channel genes representing the Shaker, Shab, Shal, and Shaw subfamilies is derived from the 18 most parsimonious trees found in a heuristic search. Numbers indicate the percentage of times a particular branch point was observed in these trees. For the unresolved branchings seen in the Shaker subfamily, no single pattern was observed in >50% of the trees from which the consensus is derived. Branches defining each subfamily are *bracketed* at the *right* edge of the figure. Shaker homologs are from rat (rKv1.1, X12589; Baumann et al., 1988), *Drosophila* (dShak, M17211; Papazian et al., 1987), *Aplysia* (aShak, M95914; Pfaffinger et al., 1991), a platyhelminth (pShak, L26968; Kim et al., 1995), and the jellyfish *Polyorchis* (jShak1 and jShak2, U32922 and U32923; Jegla et al., 1995). Shab subfamily members are from rat [rKv2.1, X16476, Frech et al. (1989); IK8 and K13, M81783 and M81784, Drewe et al. (1992)], *Drosophila* (dShab, M32659, Butler et al., 1989), and *Aplysia* (aShab, S68356, Quattrocki et al., 1994). The Shaw subfamily is represented by rKv3.1 [rat, M68880, Rettig et al. (1992)] and dShaw [*Drosophila*, M32661, Butler et al. (1989)]. The Shal subfamily includes sequences from mouse [mKv4.1, M64226, Pak et al. (1991)] and *Drosophila* [dShal, M32660, Wei et al. (1990)] as well as jShal1 and jShalγ1.

Table 2. Summary of the biophysical properties of jellyfish and *Drosophila* Shal currents

Parameter	dShal	jShal1	jShal1 + jShalγ1	jShal1 + jShalγ1 (T)
Activation				
V_{50} (mV)	−3.8 ± 0.1 (8)	−39.3 ± 0.1 (11)	−11.8 ± 0.9 (8)	−17.7 ± 0.7 (7)
Slope (mV/e-fold)	15.38 ± 0.07 (8)	22.4 ± 0.1 (11)	17.4 ± 0.1 (8)	17.5 ± 0.07 (7)
Inactivation				
V_{50} (mV)	−60.6 ± 0.1 (8)	−106.1 ± 0.2 (11)	−71.5 ± 0.2 (8)	−64.4 ± 0.7 (7)
Slope (mV/e-fold)	6.3 ± 0.1 (8)	6.1 ± 0.15 (11)	4.9 ± 0.2 (8)	7.9 ± 0.2 (7)
τ_{FAST} (msec)	40.1 ± 2.1 (8)	137 ± 6.7 (4)	2.69 ± 0.04 (13)	24.3 ± 0.8 (8)
τ_{SLOW} (msec)	165 ± 8.4 (8)	889 ± 61 (4)		275 ± 12 (8)
% Fast	57 ± 3 (8)	41 ± 2 (4)		43 ± 2 (8)
Recovery				
$\tau_{R\text{-}F}$ (msec)	505 ± 12.9 (9)	375 ± 25.4 (4)*	170 ± 5.7 (5)	9.76 ± 2.5 (7)
$\tau_{R\text{-}S}$ (msec)			3824 ± 813 (5)**	155 ± 17.2 (7)**

V_{50} and slope (in mV/e-fold change in conductance) of activation and steady-state inactivation are derived from the Boltzmann fits of the conductance/voltage and steady-state inactivation data shown in Figures 3–5. τ_{FAST} and τ_{SLOW} are the fast and slow time constants of inactivation and were determined at +50 mV. The percent of the current inactivating with τ_{FAST} is also given. $\tau_{R\text{-}F}$ and $\tau_{R\text{-}S}$ are time constants of fast and slow components of recovery from inactivation determined at −100 mV for dShal and the heteromultimeric currents and at −120 mV for jShal1. If a single component to recovery was identified, it is given as $\tau_{R\text{-}F}$. Error values (±) are for SEs of curve fits and data points, and sample sizes are indicated in parentheses.

*A small (≤15%), virtually instantaneous component to jShal1 recovery fit is not listed, because it is probably caused by channels that did not inactivate during the test pulse and did not close during the shortest recovery periods.

**These are the major recovery components for jShal1 + jShalγ1 and jShal1 + jShalγ1 (T) heteromultimers, at 87 and 64%, respectively.

inactivation time course that is relatively insensitive to voltage. However, the jShal1 current differs in two important ways. First, its inactivation rate is severalfold slower than that of dShal. Whereas the fastest inactivation time constant is ~140 msec for jShal1 at +50 mV, it is ~40 msec for dShal. Second, jShal1's activation and steady-state inactivation curves are shifted to even more hyperpolarized voltages. The V_{50} for activation of jShal1 is approximately −35 mV more hyperpolarized than that of dShal (Fig. 3*C*). The V_{50} for steady-state inactivation for jShal1 is approximately −106 mV compared with −62 mV for dShal (Fig. 3*D*).

jShalγ1 is unlike an α-subunit in that it does not form functional voltage-dependent channels when expressed as a homomultimer in *Xenopus* oocytes (Fig. 4*A*). Instead, jShalγ1 functions only in com-

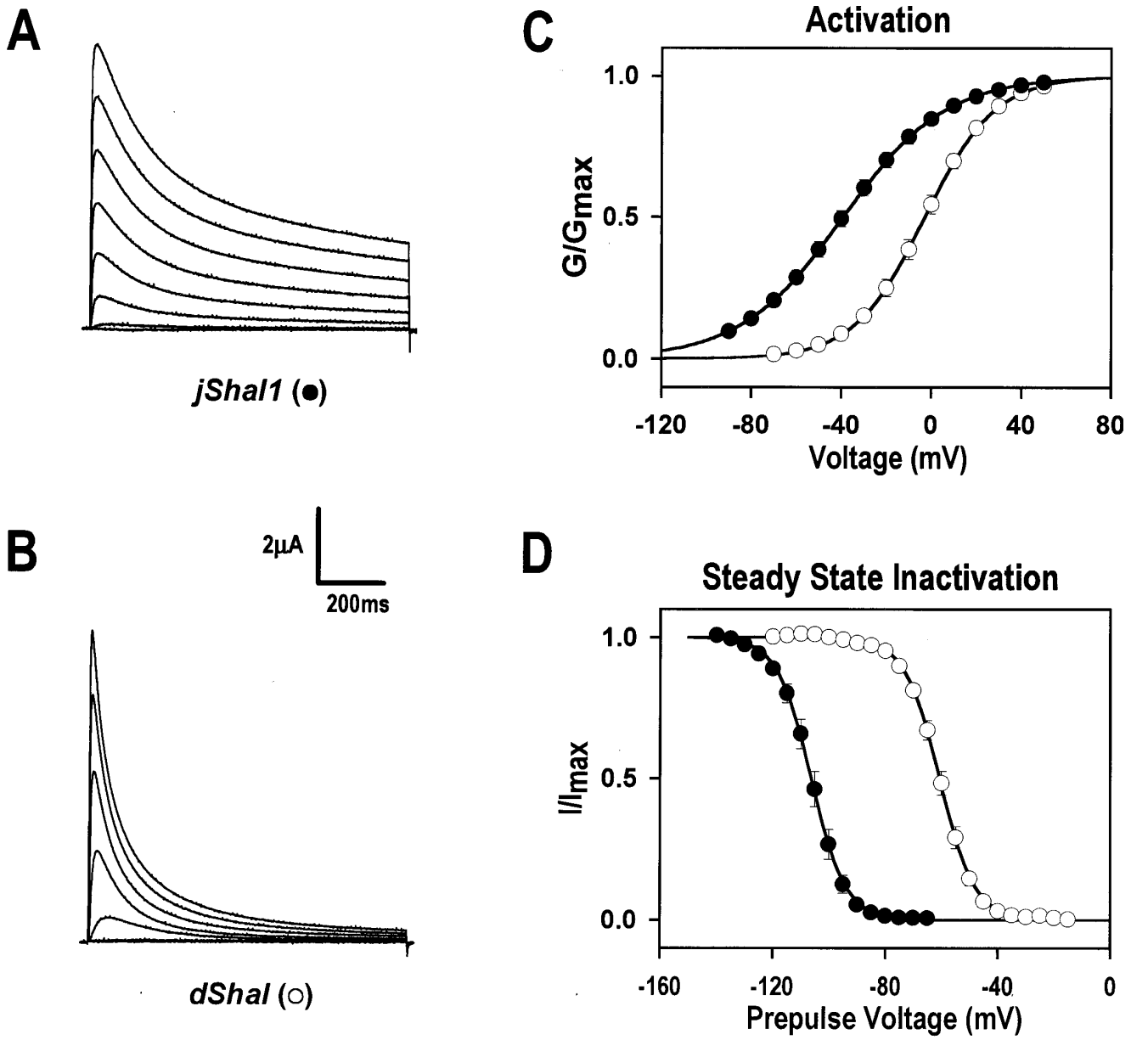

Figure 3. Comparison of the jShal1 and dShal currents. Families of outward currents are shown for *Xenopus* oocytes expressing either jShal1 (*A*) or dShal (*B*). Currents were recorded in response to 1 sec test pulses from −90 mV to +50 mV in 20 mV increments. Five second prepulses to −140 mV (from a holding potential of −90 mV) preceded each test pulse to ensure complete recovery from inactivation. *C*, Conductance versus voltage curves are shown for jShal1 (*solid circles*) and dShal (*open circles*). Error bars indicate SEM, and *solid curves* represent Boltzmann fits of the data ($G/G_{max} = 1/(1 + \exp(-(V - V_{50})/a)$, where G is the conductance at voltage V, G_{max} is the maximal conductance, V_{50} is the voltage at which $G = 0.5 \times G_{max}$, and a is the slope factor. *D*, Steady-state inactivation curves for jShal1 and dShal. Currents were obtained by measuring the peak current during test pulses to +40 mV, after 10 sec prepulses to the voltage shown on the *x*-axis. Holding potentials were −90 mV with 5 sec prepulses to −140 mV preceding test pulses. The *curves* represent best fits of the data to the Boltzmann function $I/I_{max} = 1/(1 + \exp((V - V_{50})/a)$, where I is the peak current measured during the test pulse after a prepulse to voltage V, I_{max} is the maximal current measured, V_{50} is the prepulse voltage at which $I = 0.5 \times I_{max}$, and a is the slope factor.

bination with Shal α-subunits. Figure 4*B* shows currents resulting from its co-expression with jShal1 in *Xenopus* oocytes. Because this current is distinct from jShal1 currents, it is assumed that it results from the heteromultimeric assembly of jShalγ1 and jShal1. Relative to jShal1 homomultimers, jShal1 + jShalγ1 heteromultimers inactivate much more rapidly with a time constant of <3 msec at +50 mV. This represents a several hundredfold increase in the inactivation rate from jShal1 currents (Table 2). These heteromultimeric jellyfish Shal currents resemble the majority of Shal currents expressed in *Drosophila* embryonic neurons, which inactivate with time constants near 5 msec (Tsunoda and Salkoff, 1995a). A second major change produced by the co-expression of jShalγ1 with jShal1 is a large depolarizing shift in the activation and steady-state inactivation curves compared with jShal1 (~+30 mV for activation and ~+35 mV for steady-state inactivation) (Fig. 4*C*,*D*, Table 2). Unlike jShal1 homomultimers, these heteromeric channels are much more typical of Shal channels from triploblasts with regard to their voltage range of activation.

An N-type inactivation mechanism in jShalγ1

Because jShalγ1 is unique among Shal homologs in containing a positively charged inactivation ball-like motif at its N terminal, we

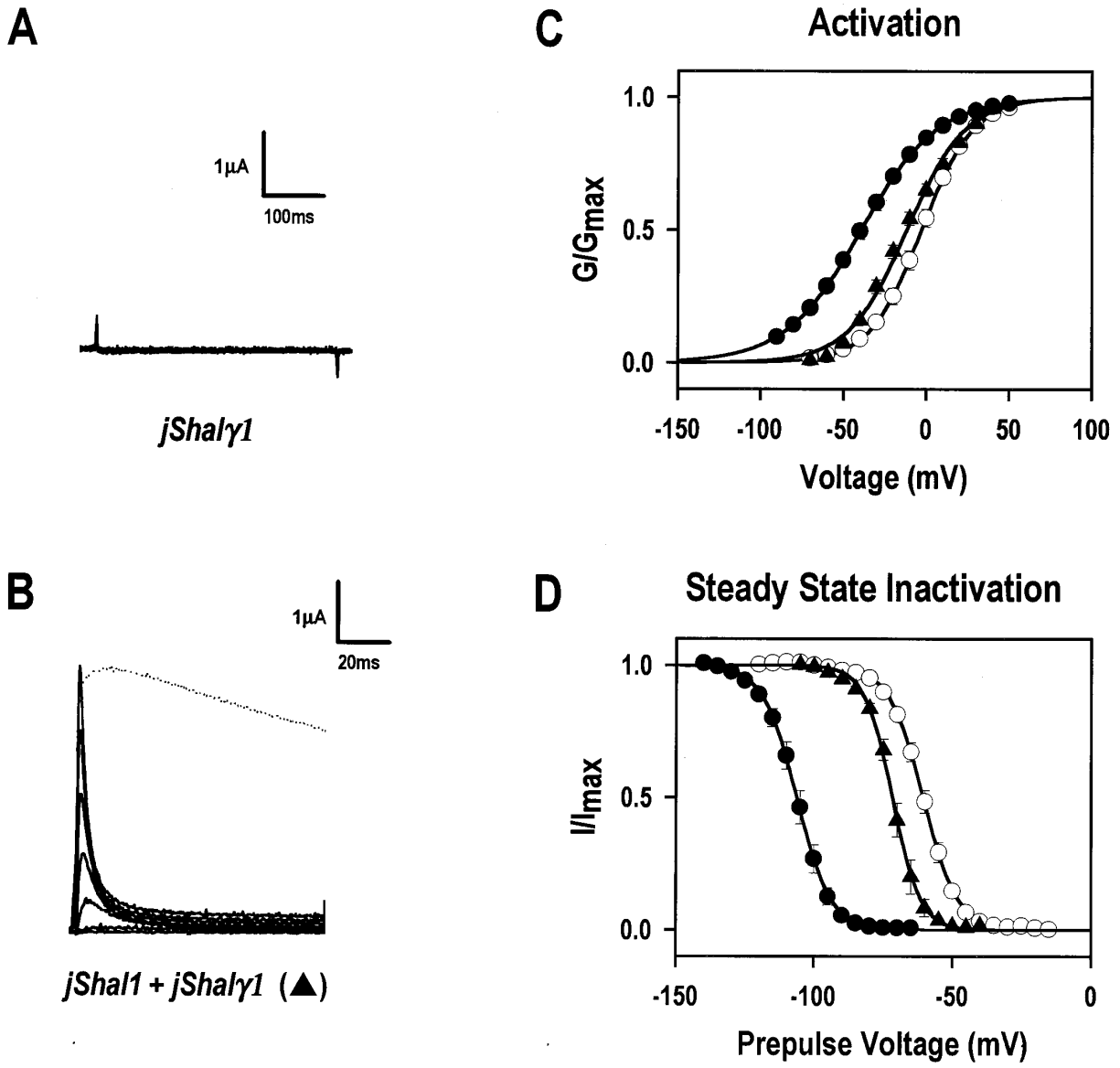

Figure 4. jShalγ1 modifies the inactivation and activation range of jShal1. *A*, Currents recorded from a *Xenopus* oocyte expressing only jShalγ1. Test pulses (400 msec) from −70 mV to +50 mV were as described in Figure 3*A*. *B*, Rapidly inactivating outward currents recorded from an oocyte co-expressing jShalγ1 and jShal1. The same voltage protocol was used, except that test pulses were 100 msec in duration. The *thin dotted line* is a jShal1 homomultimeric current (+50 mV) scaled to the same amplitude for comparison of inactivation rate. *C*, Conductance versus voltage curves for jShal1 homomultimers (*solid circles*), dShal homomultimers (*open circles*), and jShal1 + jShalγ1 heteromultimers (*solid triangles*). *D*, Steady-state inactivation curves for jShal1, dShal, and jShal1 + jShalγ1 co-injection. Data collection, analysis, and curve fitting for *C* and *D* are as in Figure 3, *C* and *D*.

tested the possibility that jShalγ1 causes rapid inactivation in jShal1 currents by contributing an N-type inactivation mechanism. To investigate this, we removed the positively charged N terminal from jShalγ1; this truncated construct is referred to here as jShalγ1(T). This N-terminal truncation does indeed result in removal of fast inactivation from the heteromultimeric current (Fig. 5*A*, Table 2), providing the first clear example of rapid N-type inactivation in Shal channels. The mechanism of N-type inactivation conferred by jShalγ1 is independent of the shift in the voltage range of activation. Thus, the activation and steady-state inactivation curves of jShal1 + jShalγ1(T) heteromultimers resemble those of jShal1 + jShalγ1 heteromultimers; both have a depolarizing shift relative to that of jShal1 homomultimers (Fig. 5*B*,*C*). Hence, this depolarized voltage range is likely to be conferred by regions other than the N terminal such as the poorly conserved regions of the jShalγ1 core. For instance, it was demonstrated that changes in the hydrophobic residues of the S4 region of Shaker can cause large shifts in the activation range (Lopez et al., 1991). Although fast N-type inactivation is absent in jShal1 + jShalγ1(T) heteromultimers, slower inactivation remains that is accelerated with respect to the inactivation of jShal1 homomultimers (Fig. 5*A*, Table 2). The residues responsible for this increased rate of residual inactivation are not known. Because N-type inactivation has been removed from jShalγ1(T), the remaining inactivation may occur by a mechanism similar to C-type inactivation in Shaker channels, which depends on residues in the P-domain and S6 (Hoshi et al., 1991, Lopez-Barneo et al., 1993).

The highly charged N-terminal domain of jShalγ1 had a profound effect on recovery from inactivation as well as on the inactivation rate. Recovery from inactivation in jShal1 + jShalγ1

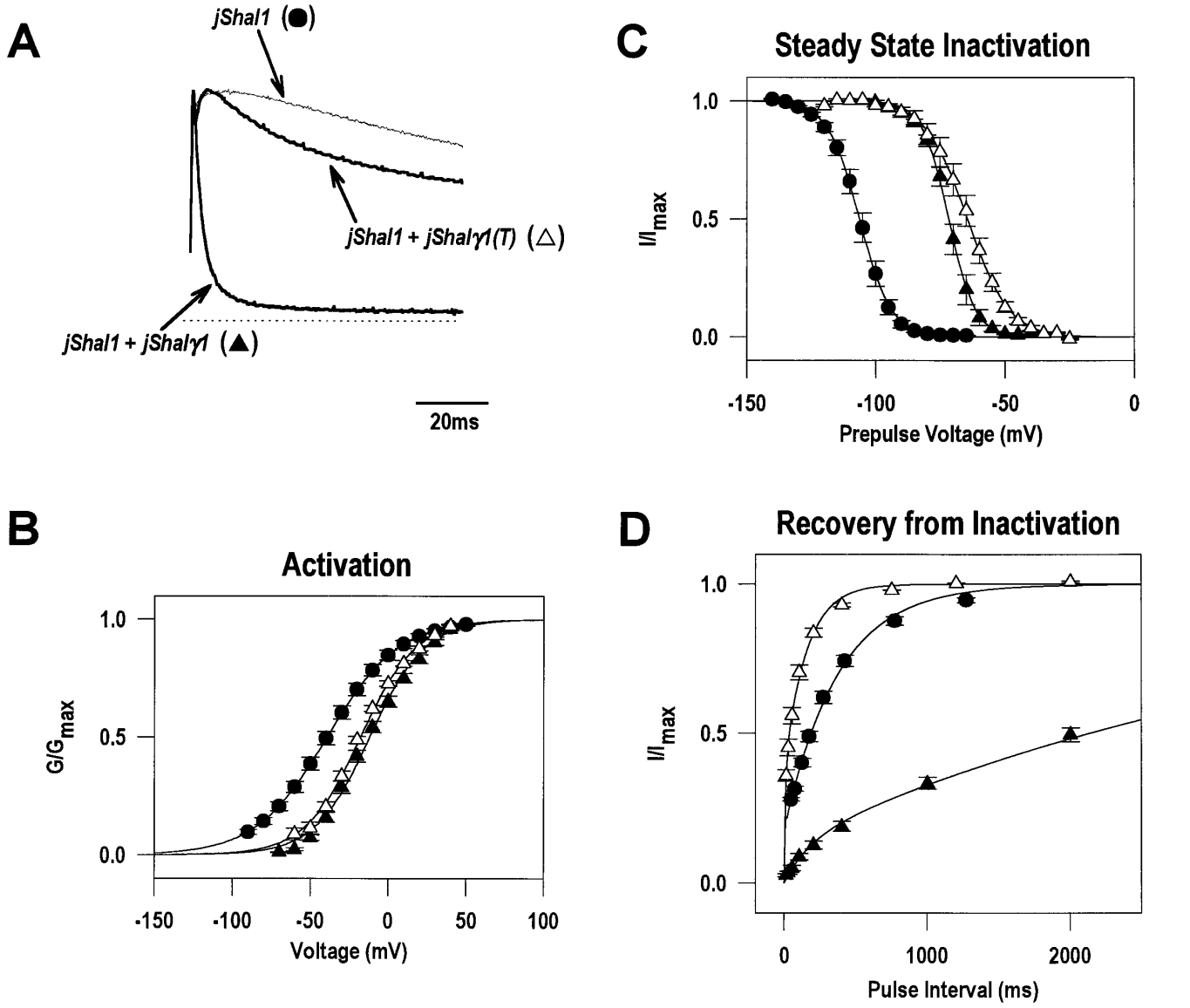

Figure 5. jShalγ1 confers rapid inactivation by an N-type mechanism. An N-terminal truncated form of jShalγ1, jShalγ1(T), was constructed by replacing the N-terminal amino acids MYSVTSTATYFLT**RK**V**K**N**R**H**R**TNVT**R**N**K** with an initiator Met. Seven positively charge residues (*bold*) that distinguish jShalγ1 from Shal α-subunits were removed. *A*, Current traces from oocytes expressing jShal1, or jShal1 + jShalγ1, or jShal1 + jShalγ1(T) recorded in response to depolarizations to +50 mV. Traces are scaled to the same amplitude for comparison of inactivation rate. *B*, Conductance voltage curves for jShal1 (*solid circles*), jShal1 + jShalγ1 (*solid triangles*), and jShal1 + jShalγ1(T) (*open triangles*). *C*, Steady-state inactivation curves for jShal1, jShal1 + jShalγ1, and jShal1 + jShalγ1(T). *D*, Time course of recovery from inactivation for jShal1, jShal1 + jShalγ1, and jShal1 + jShalγ1(T). Recovery rates were determined by a double-pulse protocol in which test pulses to +40 mV were separated by a recovery pulse of increasing duration. Recovery was at either −100 mV or −120 mV (jShal1). Because the recovery rate of all Shal channels increases with increasing hyperpolarization (T. Jegla and L. Salkoff, unpublished observations), the difference in recovery rate between jShalγ1(T) heteromultimers and jShal1 homomultimers at an identical voltage is likely to be even greater than the difference we show here. Pulse series were preceded by 5 sec prepulses to −140 mV to ensure complete recovery from inactivation. Test pulse durations were 1 sec for jShal1 and jShal1 + jShalγ1(T) and 200 msec for jShal1 + jShalγ1. Curves were generated using the equation $I_t = \{a \times (1 - \exp(-t/\tau 1))\} + \{b \times (1 - \exp(-t/\tau 2))\}$, where I_t is the current amplitude of the second +40 mV pulse divided by the current amplitude of the first pulse, t is the interval of the recovery step at −100 mV, and a and b are the components of current recovering exponentially with time constants of $\tau 1$ and $\tau 2$, respectively.

heteromultimers was measured and compared with recovery of jShal1 + jShalγ1(T) heteromultimers and jShal1 homomultimers (Fig. 5*D*). jShal1 + jShalγ1 heteromultimers recovered slowest, with a time constant of several seconds at −100 mV. However, in jShal1 + jShalγ1(T) heteromultimers, recovery is significantly more rapid and is complete within a few hundred milliseconds (Fig. 5*D*). Thus, the very slow phase of recovery from inactivation is attributable to fast N-type inactivation. On the other hand, recovery from slow "C-type" inactivation is actually faster in jShal1 + jShalγ1(T) heteromultimers than in jShal1 homomultimers (Fig. 5*D*). jShal1 recovery was measured at −120 mV instead of −100 mV because, as Figure 5*C* illustrates, most jShal1 channels are inactivated at −100 mV. jShal1 + jShalγ1 heteromultimers have a small but faster component to recovery, which may be caused by a few channels entering an alternative "C-type" inactivated state before N-type inactivation can occur. The very

Table 3. Inactivation rates of different heteromultimers containing jShalγ1

	Inactivation time constants (msec)			
	Fast	Medium*	Slow	% Fast**
jShal1 + jShalγ1	2.69 ± 0.04 (13)			Close to 100
dShal	40.1 ± 2.1 (8)		165 ± 8.4 (8)	57 ± 3 (8)
dShal1 + jShalγ1	20.2 ± 0.6 (8)		99.8 ± 5.8 (8)	59 ± 1 (8)
dShal1 + jShalγ1 (T)	44.2 ± 1.5 (7)		272 ± 8.1 (7)	44 ± 1 (7)
mShal	25.5 ± 1.0 (6)	109 ± 2.1 (6)	337 ± 13.7 (6)	19 ± 1 (6)
mShal + jShalγ1	12.3 ± 0.3 (8)	41.8 ± 1.4 (8)	228.7 ± 3.9 (8)	52 ± 2 (8)

Time constants for mShal + jShalγ1 (T) are not given because of insufficient data.

*The inactivation rate of mShal-based currents is best fit with three exponentials. The new time constant is given as "Medium."

**% Fast is the percentage of the current that inactivates with the "Fast" inactivation time constant.

slow recovery from N-type inactivation indicates that the association between the jShalγ1 inactivation ball and its blocking site on jShal1 + jShalγ1 heteromultimers is very strong.

jShalγ1 heteromultimerizes with dShal and mShal

jShalγ1 does not appear to form functional heteromultimers with α-subunits from subfamilies of voltage-gated K^+ channels other than Shal. In co-expression experiments, we found no evidence that jShalγ1 alters any biophysical properties of channels formed by the *Polyorchis* Shaker homologs jShak1 and jShak2 (data not shown). However, the ability of jShalγ1 to form heteromultimers with Shal α-subunits from other species is conserved. Evidence for this is presented in Figure 6, which shows currents resulting from the co-expression of jShalγ1 with dShal or mShal. Inactivation rates are increased when dShal and mShal are co-expressed with jShalγ1 in *Xenopus* oocytes. However, co-expression of jShalγ1 with dShal and mShal has only minor effects on the activation range, probably because homomultimeric dShal and mShal channels already operate in the voltage range in which jShalγ1 biases activation (data not shown).

Several observations suggest that the inactivation ball binding site on heteromultimers containing dShal or mShal has lower affinity for the jShalγ1 inactivation ball than the binding site on heteromultimers containing jShal1. The increase in inactivation rate in the interspecies heteromultimers is clearly caused by the N-terminal inactivation ball of jShalγ1, because inactivation is slowed if this N-terminal ball is removed (Fig. 6*A*,*B*). Nevertheless, N-type inactivation in these heteromultimers is not nearly as fast or complete as when jShalγ1 is mixed with jShal1 (Fig. 6*C*, Table 3). This shows that the Shal α-subunits, which do not have a high affinity inactivation ball themselves, contribute to the binding affinity of the jShalγ1 inactivation ball. This result is consistent with observations of the *Drosophila* Shaker channel showing that only one inactivation ball at a time is able to block the channel (MacKinnon et al., 1993). Taken together, these results suggest that N-type inactivation particles may bind to a single site formed by all four subunits (Murrell-Lagnado and Aldrich, 1993).

Stoichiometry of jShal1 + jShalγ1 heteromultimers

We have exploited the presence of the N-terminal inactivation ball on jShalγ1 to estimate the subunit stoichiometry of jShal1 + jShalγ1 heteromultimers. Our strategy was based on two assumptions. (1) The functional mechanism of N-terminal inactivation provided by jShalγ1 is the same as in Shaker N-type inactivation (MacKinnon et al., 1993). (2) jShal1 and jShalγ1 form tetrameric channels. This latter assumption is based on the structural similarity of Shal α-subunits to Shaker α-subunits, which are known to form tetramers (MacKinnon, 1991). In Shaker, the inactivation ball contributed by each of the four subunits functions independently (MacKinnon et al., 1993). This independence results in a simple additive effect of each ball on the inactivation rate. Thus, the inactivation rate of channels that have only one inactivation ball would be roughly four times slower than the inactivation rate for channels containing four inactivation balls. This result was shown by mixing increasing proportions of Shaker subunits lacking an inactivation ball with Shaker subunits having an inactivation ball. In these experiments, the inactivation rate is progressively slowed, because the number of inactivation balls per channel is progressively reduced.

Similarly, if jShal1 and jShalγ1 mix freely to produce functional heteromultimers of several stoichiometries, then increasing the proportion of jShal1 in an oocyte will progressively reduce the average number of inactivation balls on each heteromultimeric channel. This should result in slower N-type inactivation. If, on the other hand, there is only a single functional stoichiometry of jShal1 + jShalγ1 heteromultimer, then the rate of N-type inactivation should remain constant as the proportion of jShal1 is increased (while the relative amount of slowly inactivating current increases). Figure 7 illustrates this unchanging rate of fast inactivation and suggests that there is only a single functional stoichiometry in jShal1 + jShalγ1 heteromultimers. As predicted, when the amount of jShal1 is increased relative to the amount of jShalγ1, the fast-inactivating component of the current is progressively reduced, leaving a larger slow component (corresponding to the jShal1 homomultimeric current). Significantly, the time constant of fast inactivation remains unchanged.

To further investigate the stoichiometry of jShal1 + jShalγ1 heteromultimers, we co-injected jShalγ1(T), which has the inactivation ball removed, with jShal1 and jShalγ1. Unlike the previous experiment, increasing proportions of jShalγ1(T) should progressively reduce the average number of inactivation balls per heteromultimeric channel, even if the functional stoichiometry of jShalγ1 + jShal1 heteromultimers is fixed. In contrast to the experiments shown in Figure 7, the fast-inactivation rate should progressively slow. Oocytes injected with jShalγ1(T), jShalγ1, and jShal1 again had both fast- and slow-inactivating current fractions (Fig. 8). Most importantly, the rate of fast N-type inactivation is slowed almost twofold by the addition of increasing amounts of jShalγ1(T). By analogy to the Shaker results, the twofold slowing of N-type inactivation suggests that the number of inactivation balls is reduced by half when jShalγ1(T) is added. These results can be explained by postulating three

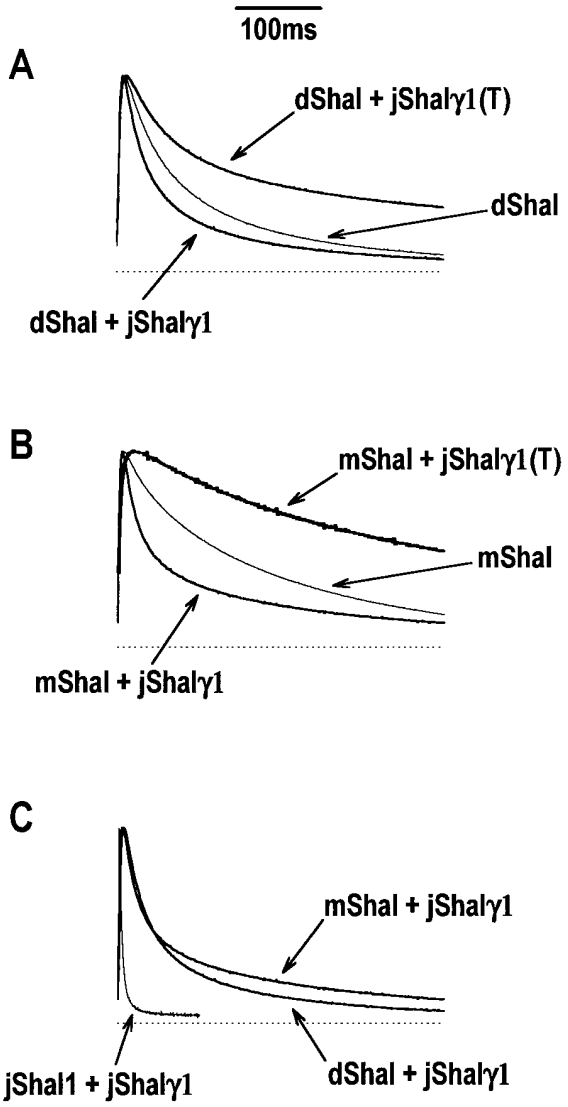

Figure 6. Heteromultimerization of jShalγ1 with dShal and mShal. *A*, Current traces recorded in response to a test pulse to +50 mV for *Xenopus* oocytes expressing dShal, dShal + jShalγ1, and dShal + jShalγ1(T) are shown normalized in amplitude for comparison of inactivation rates. *B*, Similar traces for oocytes expressing mShal, mShal + jShalγ1, and mShal + jShalγ1(T). *C*, Comparison of currents produced by co-expression of jShalγ1 + jShal1, jShalγ1 + dShal, and jShalγ1 + mShal. Although jShalγ1(T) appears to have opposite effects on the inactivation rates of dShal and mShal relative to jShal1 (Fig. 5*A*), the absolute inactivation rates of all three heteromultimers are actually quite similar.

significant current components: a very fast component produced by channels with two jShal1 and two jShalγ1-subunits, a slower "fast" component produced by channels with two jShal1, one jShalγ1, and one jShalγ1(T)-subunits, and the slow component produced by channels with two jShal1 and two jShalγ1(T)-subunits. A second slow component produced by jShal1 homomultimers is of insignificant size in these mixes, because of the high ratio of jShalγ1 and jShalγ1(T) to jShal1. Thus, it appears that heteromultimers are limited to a single stoichiometry of two jShal1-subunits and two jShalγ1-subunits (Fig. 8). The fact that we can progressively reduce the number of inactivation balls without completely removing N-type inactivation strongly supports our initial assumption that the jShalγ1 inactivation balls function independently of each other, exactly like Shaker inactivation balls.

DISCUSSION

Significance of the conservation of Shal in diploblasts

Connor and Stevens (1971b) first recognized that subthreshold A-currents have the capacity to influence neuronal firing frequency because of their active role during interspike intervals. Patterned neural output from single neurons appears to be highly conserved among animals. Neurons of diploblastic coelenterates such as *Polyorchis* are capable of firing trains of action potentials or rhythmic bursts of action potentials that are virtually indistinguishable from those of vertebrates (Anderson, 1979; Przysiezniak and Spencer, 1989). The high conservation of Shal channels is likely to be part of the reason. The conservation of several additional classes of voltage-gated ion channels also contributes to this conservation of intrinsic electrical properties between diploblastic and triploblastic neurons (Anderson and McKay, 1987; Dunlap et al., 1987; Holman and Anderson, 1991; Przysiezniak and Spencer, 1992, 1994; Anderson et al., 1993; Meech and Mackie, 1993; Jegla et al., 1995). This growing set of channels known to be shared by diploblasts and triploblasts may represent an essential set for the patterning of signals in all nervous systems and suggests that the intrinsic electrical properties of neurons were optimized early in the evolution of the nervous system.

Regulation of Shal inactivation by jShalγ1

Our finding that jShalγ1, a functionally novel Shal-subunit, regulates the inactivation rate of Shal currents parallels the discovery that β-subunits can induce rapid inactivation in *Shaker* currents (Rettig et al., 1994). In contrast to jShalγ1, these β-subunits are cytosolic proteins homologous to members of the NAD(P)H-dependent oxidoreductase superfamily (McCormack and McCormack, 1994) and are not structurally homologous to voltage-gated K^+ channel α-subunits. Although both jShalγ1 and Shaker β-subunits cause rapid inactivation by N-type mechanisms, jShalγ1 has additional effects on the voltage range of channel activation. This is, perhaps, attributable to the fact that jShalγ1 forms an integral part of the voltage-sensing mechanism of the channel.

Although jShalγ1 is similar in structure to the α-subunits of Shal and other voltage-gated K^+ channels, it is unique in that it does not form functional homomultimeric channels. Instead, it modifies the gating properties of Shal α-subunits, functioning only as a heteromultimer. This distinct functional role has led to an interesting pattern of conservation between Shal α-subunits and jShalγ1. Regions involved in subfamily-specific assembly (T1) and ion selectivity (pore region) are highly conserved, whereas regions involved in determining gating properties (N terminal, S1–S4) differ substantially.

The reason that jShalγ1 does not form functional homomultimers is not clear, but it is not exclusively attributable to constitutive inactivation resulting from the presence of four high-affinity inactivation balls. This is demonstrated by the fact that the N-terminal truncated construct jShalγ1(T) also fails to express a voltage-dependent current as a homomultimer. The unusually short C-terminal cytoplasmic domain is also unlikely to be responsible for the failure of homomultimer formation. This was shown by substituting the longer C-terminal domain of jShal1 for the shorter C-terminal domain of jShalγ1; expression of voltage-dependent currents was not recovered (data not shown). These

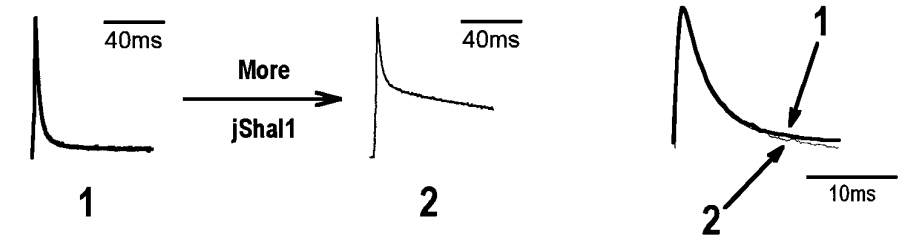

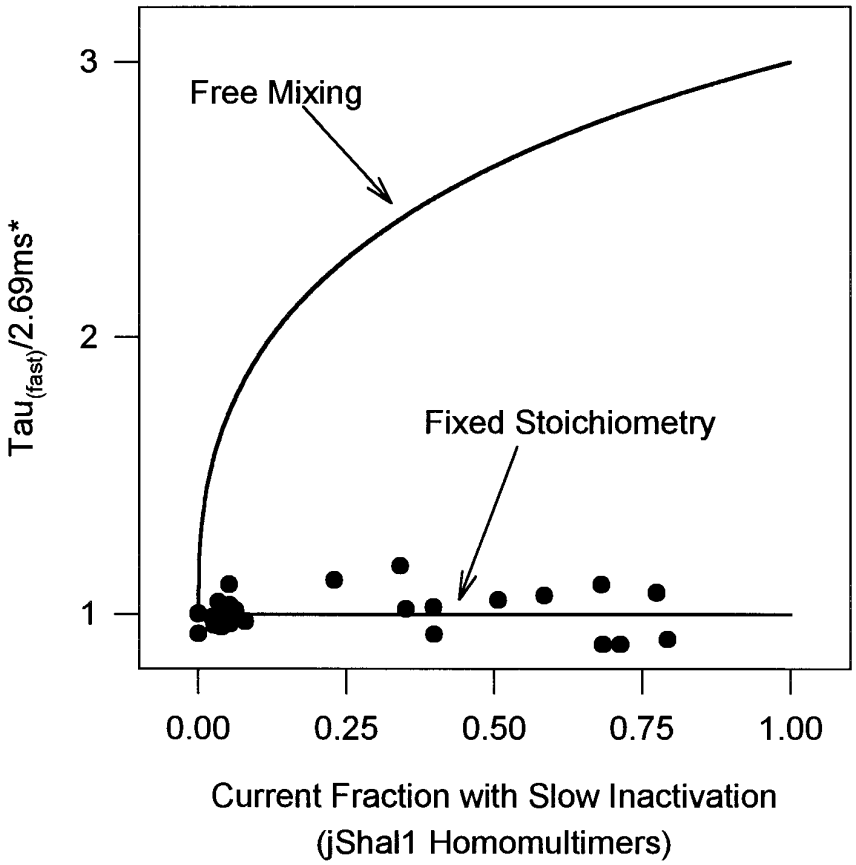

Figure 7. jShal1 and jShalγ1 form functional channels in a single stoichiometry. *1* and *2* show current traces (normalized in amplitude) for oocytes expressing jShal1 + jShalγ1 in a jShalγ1-biased mix (*1*) or a jShal1-biased mix (*2*). The large, slowly inactivating component in *2* has the properties of a jShal1 homomultimer current. On the *right*, the fast-inactivating components of *1* and *2* have been normalized to the same amplitude and plotted together, showing nearly identical inactivation rates. The graph shows a plot of the fast-inactivation time constant versus fraction of the total current with slow inactivation (jShal1 homomultimeric current) for individual experiments in which oocytes were injected with varying ratios of jShal1 and jShalγ1 (*solid circles*). The time constants are normalized to the mean fast-inactivation time constant calculated from the leftmost group of data points (2.69 msec), representing jShalγ1-biased mixes in which virtually no slowly inactivating current is seen. Inactivation rate was not increased by further biasing the ratio toward jShalγ1. The *straight line* (*Fixed Stoichiometry*) indicates the predicted relationship between the fast-inactivation time constant and the fraction of current with slow inactivation if only a single stoichiometry of heteromultimer is functional. The *curve* (*Free Mixing*) represents the prediction of fast-inactivation time constant if jShal1 and jShalγ1 form functional channels in all possible stoichiometries.

experiments strongly imply that jShalγ1 is specifically designed to function only in a heteromultimeric configuration.

The restriction of functional jShal1 + jShalγ1 heteromultimers to a single 2:2 functional stoichiometry may be necessary to precisely fix the voltage range and inactivation rate of the current rather than to allow gradations of these properties. Because the jShalγ1 inactivation ball binding site appears to involve both the jShal1 and jShalγ1-subunits, a precise arrangement of these two types of subunits may be necessary to produce a high-affinity binding site. If so, only one of two possible arrangements of the two jShalγ1-subunits within the 2:2 heteromultimers (side by side or opposite) may produce functional fast-inactivating channels. It may be possible to address this question in the future by using tandem constructs of jShalγ1 and jShal1. If both arrangements are functional, fast-inactivating heteromultimers should be obtained by expression of jShalγ1 + jShal1 dimers (opposite arrangement) as well as by co-expression of jShalγ1 + jShalγ1 and jShal1 + jShal1 dimers (side by side arrangement). We do not know whether 3:1 and 1:3 stoichiometries of jShal1 + jShalγ1 heteromultimers assemble but are nonfunctional or simply do not assemble.

In addition to jShalγ1, three other K^+ channel subunits have been isolated that appear to belong to a specific voltage-gated K^+ channel subfamily but do not express currents as homomultimers: IK8 and K13 from rat (Drewe et al., 1992) and nShaw1 from the nematode *Caenorhabditis elegans* (Dr. Aguan Wei, personal communication). IK8 and K13 are more closely related to the Shab subfamily, whereas nShaw1 is a Shaw homolog. Although no functional link between these subunits and any Shab or Shaw α-subunits has yet been established, it is conceivable that these could be similar γ-subunits for the Shab and Shaw subfamilies. Similar subunits have been found for cyclic nucleotide-gated channels (Bradley et al., 1994; Liman and Buck, 1994) and for inward rectifier K^+ channels (Krapivinsky et al., 1995). Such "regulatory" subunits may turn out to be common but have simply been difficult to clone and characterize by traditional

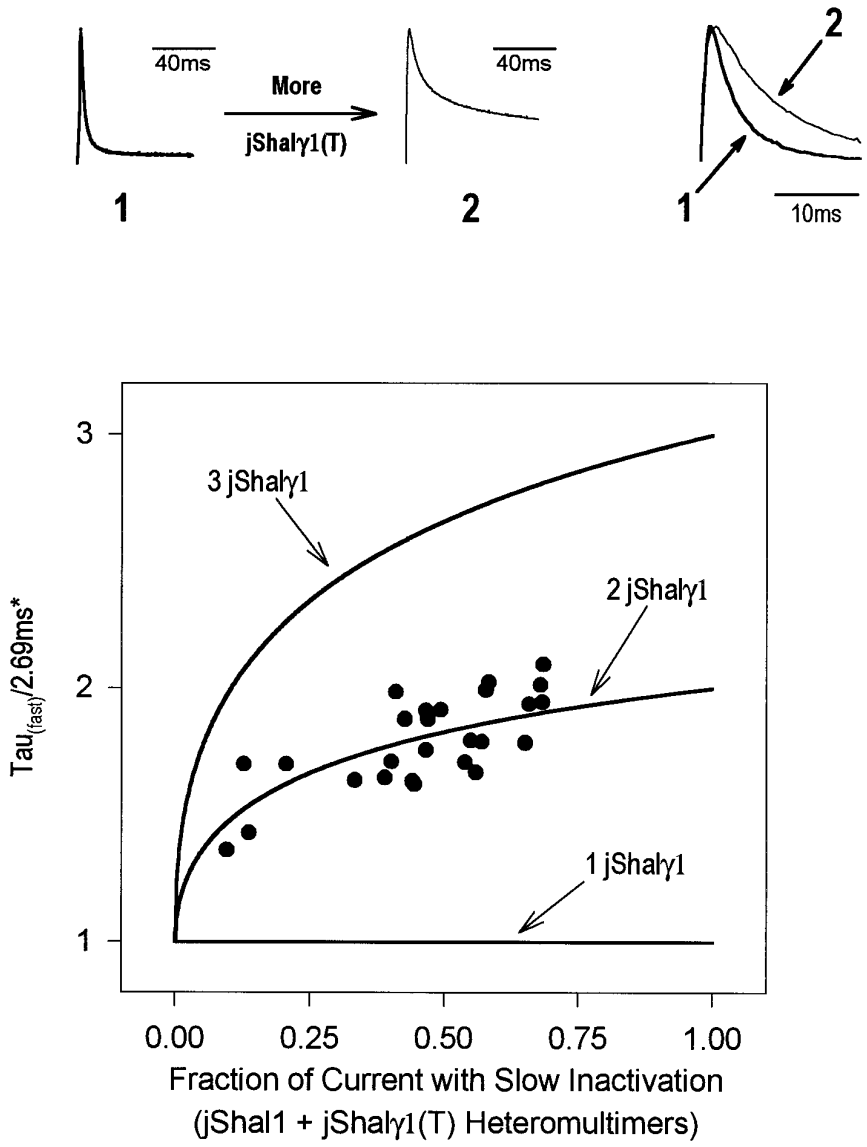

Figure 8. Functional jShal1–jShalγ1 heteromultimers have a 2:2 stoichiometry. *1* and *2* show currents (normalized in amplitude) from an oocyte expressing only jShal1 + jShalγ1 (*1*) and an oocyte expressing jShal1 + jShalγ1 + jShalγ1(T) (*2*) [jShalγ1 and jShalγ1(T) are in a 1:1 ratio]. The slowly inactivating current fraction is almost completely produced by jShal1 + jShalγ1(T) heteromultimers. jShal1 homomultimers contribute little to this slow current, because cRNA mixes were biased toward jShalγ1 + jShalγ1(T). Therefore, the inactivation time constants and steady-state inactivation curves for slowly inactivating fractions closely matched the inactivation time constants of jShal1 + jShalγ1(T) heteromultimers. The traces on the *right* show a comparison of the fast-inactivating fractions of *1* and *2* normalized to the same amplitude. This shows that adding jShalγ1(T) slows N-type inactivation. The graph shows predictions of the fast-inactivation time constant versus fraction of slowly inactivating current, in which the functional heteromultimeric channels contain either 1, 2, or 3 jShalγ1-based-subunits. *Solid circles* represent data from individual experiments; the fit assumes two jShalγ1-subunits in the functional heteromultimers.

methods because of their sequence divergence and inability to function independently.

Because the functional expression of jShalγ1 appears to depend on co-expression with jShal1 α-subunits, both must be expressed in the same cells for either to have functional significance. [Most homomultimeric jShal1 channels would be inactivated at the resting potentials of all *Polyorchis* cells described so far (Przyiezniak and Spencer, 1989).] Because of this apparent functional interdependence, it seems likely that both are expressed in the same cells, but an additional possibility is that jShalγ1 co-assembles with an as yet unknown *Polyorchis* Shal α-subunit. Although we have not verified that jShalγ1 and jShal1 are expressed in the same cells in *Polyorchis*, we do know that both are present in the same neuronally enriched cDNA libraries (Gallin, 1991).

Are jShalγ1 homologs present in triploblasts?

Because *Shal* subfamily K^+ channel genes are so highly conserved, it is plausible that triploblasts will be found to have homologs of jShalγ1. Indeed a physiological role for such homologs has been tentatively identified. The fast-inactivating Shal currents found in *Drosophila* neurons (Tsunoda and Salkoff, 1995a) are much more similar to jShal1 + jShalγ1 heteromultimeric currents than to the homomultimeric currents expressed by *dShal* in *Xenopus* oocytes. Similar γ-subunits could also explain the faster inactivation and altered activation range of Shal currents produced by co-expression of mammalian Shal channels with the 2–4 kb fraction of brain mRNA (Chabala et al., 1993; Serodio et al., 1994). Significantly, jShalγ1 forms functional heteromultimers with both dShal and mShal. This shows that the ability of Shal α-subunits to co-assemble with Shal γ-subunits has been conserved throughout metazoan evolution. Thus, jShalγ1 may represent a conserved molecular mechanism for regulating neuronal firing rate.

REFERENCES

Anderson PAV (1979) Ionic basis of action potentials and bursting activity in the hydromedusan jellyfish *Polyorchis penicillatus*. J Exp Biol 78:299–302.

Anderson PAV, McKay MC (1987) The electrophysiology of cnidocytes. J Exp Biol 133:215–230.

Anderson PAV, Holman MA, Greenberg RM (1993) Deduced amino acid sequence of a putative sodium channel from the scyphozoan jellyfish *Cyanea capillata*. Proc Natl Acad Sci USA 90:7419–7423.

Baumann A, Grupe A, Ackermann A, Pongs O (1988) Structure of the voltage-dependent potassium channel is highly conserved from *Drosophila* to vertebrate central nervous systems. EMBO J 7:2457–2463.

Bradley J, Li J, Davidson N, Lester HA, Zinn K (1994) Heteromeric olfactory cyclic nucleotide-gated channels: a subunit that confers increased sensitivity to cAMP. Proc Natl Acad Sci USA 91:8890–8894.

Butler A, Wei A, Baker K, Salkoff L (1989) A family of putative potassium channel genes in *Drosophila*. Science 243:943–947.

Chabala LD, Bakry N, Covarrubias M (1993) Low molecular weight poly(A)$^+$ mRNA species encode factors that modulate gating of a non-Shaker A-type K^+ channel. J Gen Physiol 102:713–728.

Connor JA, Stevens WF (1971a) Voltage clamp studies of a transient outward membrane current in gastropod neural somata. J Physiol (Lond) 213:21–30.

Connor JA, Stevens WF (1971b) Prediction of repetitive firing behavior from voltage clamp data on an isolated neurone soma. J Physiol (Lond) 213:31–53.

Covarrubias M, Wei A, Salkoff L (1991) Shaker, *Shal*, *Shab* and *Shaw* express independent K^+ current systems. Neuron 7:763–773.

Drewe J, Verma S, Frech G, Joho R (1992) Distinct spatial and temporal expression patterns of K^+ channel mRNAs from different subfamilies. J Neurosci 12:538–548.

Dunlap K, Takeda P, Brehm P (1987) Activation of a calcium-dependent photoprotein by chemical signaling through gap junctions. Nature 325:60–62.

Frech GC, VanDongen AMJ, Schuster G, Brown AM, Joho RH (1989) A novel K^+ channel with delayed rectifier properties isolated from rat brain by expression cloning. Nature 340:642–645.

Gallin WJ (1991) Sequence of an acidic ribosomal protein from the jellyfish *Polyorchis penicillatus*. Biochem Cell Biol 69:211–215.

Hartmann HA, Kirsch GE, Drewe JA, Taglialatela M, Joho RH, Brown AM (1991) Exchange of conduction pathways between two related K^+ channels. Science 251:942–944.

Ho SN, Hunt HD, Horton RM, Pullen JK, Pease LR (1989) Site-directed mutagenesis by overlap extension using the polymerase chain reaction. Gene 77:51–79.

Holman M, Anderson PAV (1991) Voltage-activated ionic currents in myoepithelial cells from the sea anemone *Calliactis tricolor*. J Exp Biol 161:333–346.

Hoshi T, Zagotta WN, Aldrich RW (1990) Biophysical and molecular mechanisms of *Shaker* potassium channel inactivation. Science 250:533–538.

Hoshi T, Zagotta WN, Aldrich RW (1991) Two types of inactivation in *Shaker* K^+ channels: effects of alterations in the carboxy-terminal region. Neuron 7:547–556.

Jegla T, Salkoff L (1995) A multigene family of novel K^+ channels from *Paramecium tetraurelia*. Receptors Channels 3:51–60.

Jegla T, Grigoriev N, Gallin WJ, Salkoff L, Spencer AN (1995) Multiple *Shaker* potassium channels in a primitive metazoan. J Neurosci 15:7989–7999.

Kim E, Day TA, Bennett JL, Pax RA (1995) Cloning and functional expression of a *Shaker*-related voltage-gated potassium channel gene from the flatworm *Schistosoma mansoni* (Trematoda: Digenea) J Parasitol 20:171–180.

Kozak M (1987) At least six nucleotides preceding the AUG initiator codon enhance translation in mammalian cells. J Mol Biol 196:947–950.

Krapivinsky G, Gordon EA, Wickman K, Velimirovic B, Krapivinsky L, Clapham DE (1995) The G-protein-gated atrial K^+ channel I_{KACh} is a heteromultimer of two inwardly rectifying K^+ channel proteins. Nature 374:135–141.

Li M, Jan YN, Jan LY (1992) Specification of subunit assembly by the hydrophilic amino-terminal domain of the *Shaker* potassium channel. Science 257:1225–1230.

Liman ER, Buck LB (1994) A second subunit of the olfactory cyclic nucleotide-gated channel confers high sensitivity to cAMP. Neuron 13:611–621.

Lopez GA, Jan YN, Jan LY (1991) Hydrophobic substitution mutations in the S4 sequence alter voltage-dependent gating in Shaker K^+ channels. Neuron 7:327–336.

Lopez-Barneo J, Hoshi T, Heinemann SH, Aldrich RW (1993) Effects of external cations and mutations in the pore region on C-type inactivation of *Shaker* potassium channels. Receptors Channels 1:61–71.

MacKinnon R (1991) Determination of the subunit stoichiometry of a voltage-activated K^+ channel. Nature 350:232–235.

MacKinnon R, Aldrich RW, Lee A (1993) Functional stoichiometry of Shaker K^+ channel inactivation. Science 262:757–759.

McCormack T, McCormack K (1994) Shaker K^+ channel beta subunits belong to an NAD(P)H-dependent oxidoreductase superfamily. Cell 79:1133–1135.

Meech RW, Mackie GO (1993) Potassium channel family in the giant motor axons of *Aglantha digitale*. J Neurophysiol 69:894–901.

Morris SC (1993) The fossil record and the early evolution of the Metazoa. Nature 361:219–225.

Murrell-Lagnado RD, Aldrich RW (1993) Interactions of amino terminal domains of Shaker K channels with a pore blocking site studied with synthetic peptides. J Gen Physiol 102:949–975.

Ochman H, Gerber AS, Hartl DL (1988) Genetic applications of an inverse polymerase chain reaction. Genetics 120:621–625.

Pak MD, Baker K, Covarrubias M, Butler A, Ratcliffe A, Salkoff L (1991) mShal, a subfamily of A-type K^+ channel cloned from mammalian brain. Proc Natl Acad Sci USA 88:4386–4390.

Papazian DM, Schwarz TL, Tempel BL, Jan YN, Jan LY (1987) Cloning of genomic and complementary DNA from *Shaker*, a putative potassium channel gene from *Drosophila*. Science 237:749–753.

Papazian DM, Timpe LC, Jan YN, Jan LY (1991) Alteration of voltage-dependence of *Shaker* potassium channel by mutations in the S4 sequence. Nature 349:305–310.

Pfaffinger PJ, Furukawa Y, Zhao B, Dugan D, Kandel ER (1991) Cloning and expression of an *Aplysia* K^+ channel and comparison with native *Aplysia* K^+ currents. J Neurosci 11:918–927.

Przysiezniak J, Spencer AN (1989) Primary culture of identified neurones from a Cnidarian. J Exp Biol 142:97–113.

Przysiezniak J, Spencer AN (1992) Voltage-activated calcium currents in identified neurons from a hydrozoan jellyfish, *Polyorchis penicillatus*. J Neurosci 12:2065–2078.

Przysiezniak J, Spencer AN (1994) Voltage-activated potassium currents in isolated motor neurons from the jellyfish *Polyorchis penicillatus*. J Neurophysiol 72:1010–1019.

Quattrocki EH, Marshal J, Kaczmarek LK (1994) A *Shab* potassium channel contributes to action potential broadening in peptidergic neurons. Neuron 12:73–86.

Rettig J, Wunder F, Stocker M, Lichtinghagen R, Mastiaux F, Beckh S, Kues W, Pedarzani P, Schroter KH, Ruppersberg JP, Veh R, Pongs O (1992) Characterization of a *Shaw*-related potassium channel family in the brain. EMBO J 11:2473–2486.

Rettig J, Heinemann SH, Wunder F, Lorra C, Parcej DN, Dolly JO, Pongs O (1994) Inactivation properties of voltage-gated K^+ channels altered by presence of a β-subunit. Nature 369:289–294.

Salkoff L, Baker K, Butler A, Covarrubias M, Pak MD, Wei A (1992) An essential set of K^+ channels conserved in flies, mice and humans. Trends Neurosci 15:161–166.

Serodio P, Kentros C, Rudy B (1994) Identification of molecular components of A-type channels activating at subthreshold potentials. J Neurophysiol 72:1516–1529.

Shen NV, Pfaffinger PJ (1995) Molecular recognition and assembly sequences involved in the subfamily-specific assembly of voltage-gated K^+ channel subunit proteins. Neuron 14:625–633.

Shen NV, Chen X, Boyer MM, Pfaffinger PJ (1993) Deletion analysis of K^+ channel assembly. Neuron 11:67–76.

Sheng M, Tsaur M-L, Jan YN, Jan LY (1992) Subcellular segregation of two A-type K^+ channel proteins in rat central neurons. Neuron 9:271–284.

Swofford DL (1993) Phylogenetic analysis using parsimony. Illinois Natural History Survey. Champaign, IL.

Tsunoda S, Salkoff L (1995a) Genetic Analysis of *Drosophila* neurons: *Shal*, *Shaw* and *Shab* encode most embryonic potassium currents. J Neurosci 15:1741–1754.

Tsunoda S, Salkoff L (1995b) The major delayed rectifier in both *Drosophila* neurons and muscle is encoded by *Shab*. J Neurosci 15:5209–5221.

Wei A, Covarrubias M, Butler A, Baker K, Pak M, Salkoff L (1990) Diverse K^+ currents expressed by a *Drosophila* extended gene family which is conserved in mouse. Science 248:599–603.

Wei A, Solaro C, Lingle C, Salkoff L (1994) Calcium sensitivity of BK-type K_{ca} channels determined by a separable domain. Neuron 13:671–681.

Yool AJ, Schwarz TL (1991) Alteration of ionic selectivity of a K^+ channel by mutation of the H5 region. Nature 349:700–704.

Zagotta WN, Hoshi T, Aldrich RW (1990) Restoration of inactivation in mutants of *Shaker* potassium channels by a peptide derived from *ShB*. Science 250:568–571.